Soil Use and Management

Soil Use and Management, March 2014, **30,** 99–108 doi: 10.1111/sum.12098

Modeling within field variation of the compaction layer in a paddy rice field using a proximal soil sensing system

M. M. Islam, T. Saey, P. De Smedt, E. Van De Vijver, S. Delefortrie & M. Van Meirvenne
Research Group Soil Spatial Inventory Techniques, Department of Soil Management, Faculty of Bioscience Engineering, Ghent University, Coupure 653, 9000 Gent, Belgium

Abstract

A key characteristic of flooded paddy fields is the plough pan. This is a sub-soil layer of greater compaction and bulk density, which restricts water losses through percolation. However, the thickness of this compacted layer can be inconsistent, with consequences such as variable percolation and leaching losses of nutrients, which therefore requires precision management of soil water. Our objective was to evaluate a methodology to model the thickness of the compacted soil layer using a non-invasive electromagnetic induction sensor (EM38-MK2). A 2.7 ha alluvial non-saline paddy rice field was measured with a proximal soil sensing system using the EM38-MK2 and the apparent electrical conductivity (EC_a) of the wet paddy soil was recorded at a high-resolution (1.0 × 0.5 m). Soil bulk density (n = 10) was measured using undisturbed soil cores, which covered locations with large and small EC_a values. At the same locations (within 1 m^2) the depth of the different soil layers was determined by penetrometer. Then a fitting procedure was used to model the EC_a – depth response functions of the EM38-MK2, which involved solving a system of non-linear equations and a R^2 value of 0.89 was found. These predictions were evaluated using independent observations (n = 18) where a Pearson correlation coefficient of 0.87 with an RMSEE value of 0.03 m was found. The EC_a measurements allowed the detail estimation of the compacted layer thickness. The link between water percolation losses and thickness of the compacted layer was confirmed by independent observations with an inverse relationship having a Pearson correlation coefficient of 0.89. This rapid, non-invasive and cost-effective technique offers new opportunities to measure differences in the thickness of compacted layers in water-saturated soils. This has potential for site-specific soil management in paddy rice fields.

Keywords: Apparent electrical conductivity, compaction thickness, EM38-MK2, modeling, paddy, water management

Introduction

In the intensive paddy rice cultivation system the fields are kept flooded for the greater part of the growing season. During land preparation, the water-saturated fields are ploughed i.e. puddled at the same depth. Commonly reported puddling depth used in floodplain paddy fields is about 0.16 m (De Datta, 1981). Repeated puddling creates a physical soil compaction beneath the puddled soil. This compaction forms a distinct high-density soil layer known as the plough pan (McDonald *et al.*, 2006), which limits water percolation beyond the rooting zone and keeps the fields under water during the growing season. Soil beneath this plough pan, on the other hand, remains unaffected from tillage induced influences of soil compaction. The soil of a puddled paddy field can thus be presented as a layered system where the plough pan is the compacted layer and has a distinctly different density than the soil above and below it.

Although puddling is homogeneously practiced within a given paddy field, the vertical extent of the compacted soil layer can vary across the field. As this layer is required to restrict water losses through percolation and nutrient losses through leaching (Kukal & Sidhu, 2004) variation in its thickness can adversely affect the site-specific soil management. The consequences thereof only become clear when dry zones emerge across the field as a result of

Correspondence: M. M. Islam. E-mail: mohammadmonirul.islam@ugent.be
Received August 2012; accepted after revision November 2013

unexpected water loss. Adjusting soil management practices to correct for the compaction problem is impossible once the crop is already planted. Therefore; the thickness of the compacted layer should be determined prior to paddy planting. This can then allow optimizing the resource use efficiency, yield stability and productivity in the paddy rice cultivation system. Precise information on the depth of compacted soil layer should be the basis of a more precise management of paddy rice fields.

Soil compaction is indicated by an increase in soil density, but measuring soil bulk density differences consistently with increasing soil depth is difficult. Using typical bulk density samplers with corers or rings, it is not feasible to sample the saturated paddy soils under crop growing conditions. Since a penetrometer measures soil resistance caused by an increase in soil density (Perumpral, 1987) it allows to measure soil compaction (Reintam *et al*., 2009) in a saturated field. Penetrometers are also useful in finding hard layers that obviously can obstruct water flow through a soil (Motavalli *et al*., 2003). However, penetrometer measurements can only be taken at point locations. This limits the possibility to obtain continuous information about soil compaction. Therefore, non-invasive proximal soil sensing techniques allowing acquisition of high-resolution soil information offer an alternative (Hoefer *et al*., 2010). A mobile proximal sensing system employing electromagnetic induction (EMI) can measure the apparent electrical conductivity (EC_a) of the soil without having a direct physical contact with the soil (McNeill, 1980). The high-resolution information obtained from a non-invasive EMI sensor can be interpreted to explain the variation of soil properties (Sudduth *et al*., 1997) such as salinity (Triantafilis *et al*., 2000), texture (Saey *et al*., 2009a), clay mineralogy (Sudduth *et al*., 2005), compaction (Brevik & Fenton, 2004), temperature (Sheets & Hendrickx, 1995) and organic carbon (Simbahan *et al*., 2006; Martinez *et al*., 2009). Rhoades *et al*. (1989) developed a bulk EC_a model of soil, which could be used to evaluate the effect of a change in several soil properties on EC_a under unsaturated field conditions. Under non-saline and saturated soil conditions, the influence of salinity and moisture variations on the sensor signal is eliminated (Islam *et al*., 2012). Thus in soils having a low variation in clay content, it is mainly the soil compaction or pore volume variation (Rhoades *et al*., 1999), and depth to contrasting soil layers (Saey *et al*., 2008, 2012) that contribute to the EC_a variability. Thus in a puddled paddy field environment, variations in EC_a can reflect changes in soil compaction. However, no report is currently available on the non-invasive measurements of within-field spatial variability of soil compaction in paddy field conditions.

The main objective of this study was to evaluate a methodology for determining the variation in the thickness of the compacted layer within a paddy field using a mobile soil sensing system. This required (i) characterizing paddy field using EC_a measurements under saturated conditions, (ii) modeling and validating the relationship between EC_a and thickness of the compacted layer, and (iii) interpreting the thickness differences in terms of soil-water percolation.

Materials and methods

Study site

A 2.7 ha experimental paddy field located at the Bangladesh Agricultural University, Mymensingh, Bangladesh, central co-ordinates 24.72450°N and 90.42317°E, was selected for this study. The field lies about 8 m above the mean sea level and has a traditional paddy cultivation history of more than five decades. The soil of the field was developed on the alluvial deposits of the Brahmaputra and consists of fine sand to silty material (Aeric Haplaquepts). A soil survey reported that the mean electrical conductivity of the puddled layer is 8.1 ± 0.8 mS/m (Brammer, 1996). However, this laboratory measured EC_e (of saturated soil paste) is different than the field measured EC_a since the EC_a measurements are taken *in situ*. Brammer (1981) reported that these alluvial floodplain soils are generally non-saline. Every growing season the field is flooded and subsequently puddled before planting of paddy rice.

Sampling the soil layers

A transect (AB) was laid out (N-S oriented) covering the length of the field (Figure 3a). Along AB three replicates of 10 undisturbed soil samples were taken within 1 m^2 at three depths (0–0.15, 0.15–0.30 and 0.30–0.45 m). The oven dried (105 °C) weight of the soil samples and the known volume of the sampling cores (0.75 L) were used to calculate soil bulk density. These bulk density measurements were done under dry field condition in June 2011, which is the commonly used procedure for taking bulk density samples using Kopecki rings.

The field was afterwards saturated with water and puddled as is commonly practiced for paddy rice planting. At the previous ten sampling locations along transect AB (Figure 3a), soil penetration resistance (PR) was measured by an SC900 soil compaction meter (Spectrum Technologies Inc., IL, USA). Along a separate transect CD, measurements of PR were also taken at 18 locations (Figure 3c). During measurement, PR readings up to a depth of 0.45 m at every 0.025 m depth interval were recorded. At each location three readings were taken within 1 m^2 and averaged. The penetrometer has a 30° conical probe with 12.82 mm diameter and was equipped with an ultrasonic depth sensitivity sensor (ASABE standards, 2011). PR (in kPa) was measured by an internal load cell and information saved by the data logging system.

Soil electrical conductivity (EC) measurements were also taken at each of the previous ten sampling locations along AB with a FieldScout direct soil EC meter (Spectrum Technologies Inc.). Three replicated measurements covering 1 m^2 per location were taken from the puddled layer (0–0.16 m). The stainless steel probe was inserted directly into the soil at 0.08 and 0.16 m depths and the average EC was calculated to derive a representative value for 0–0.16 m layer.

The soil sensing system

A mobile proximal soil sensing system (Islam & Van Meirvenne, 2011) was used to acquire high-resolution soil EC_a data on flooded paddy field conditions. In the system, the EM38-MK2 (Geonics Limited, Canada) EMI soil sensor is placed inside a waterproof housing. The sensor is non-invasive hence, does not require a direct ground contact to obtain soil information (Figure 1). The system is equipped with a DGPS receiver with a pass to pass accuracy of ± 0.20 m and pulled by a tractor. Geo-referenced EC_a data acquired by the system were logged and processed *in-situ* in a field laptop.

The EM38-MK2 records the soil EC_a at a particular location. The sensor consists of one transmitter coil and two receiver coils from which measurements can be taken every second. The receiver coils are at 0.5 and 1.0 m distances from the transmitter coil. Both the horizontal (H.5 and H1) and vertical orientations (V.5 and V1) of the sensor can be used to collect EC_a measurements. Operating the sensor hence in different coil orientations provides measurements with a different depth response. Thus these different coil orientations allow the detection of conductivity variations over different soil layers. The depth below the sensor at which 70% of the cumulative influence of the signal is obtained is conventionally used as the theoretical depth of influence – DOI (Van Meirvenne *et al.*, 2013). The DOIs of the four configurations are: 0.38 m for the H.5 orientation, 0.75 m for both the H1 and V.5 orientations, and 1.50 m for the V1 orientation. Each orientation has a different distribution of the depth sensitivity. Hence, both the inter-coil spacing and the coils orientation of the sensor are used to resolve the multi-layered soil configuration (McNeill, 1980).

To obtain detailed soil EC_a information after puddling, the water saturated paddy field was surveyed two times on two consecutive days in July 2011, using H on the first and V on the second day. As such four EC_a data sets were obtained: H.5 and H1 in horizontal, and V.5 and V1 in vertical orientations. During both surveys, measurements were taken along 1 m apart parallel lines by maintaining a resolution of 0.5 m within a line. All collected EC_a measurements were standardized to a reference temperature of 25 °C according to Sheets & Hendrickx (1995):

$$EC_{a_{25}} = EC_{a_{obs}}\left(0.4470 + 1.4034.e^{-T/26.815}\right) \quad (1)$$

with $EC_{a_{25}}$ being the standardized EC_a at 25 °C and ECa_{obs} the EC_a values at soil temperature T (°C). During the survey T was recorded by a bimetal sensor pushed in the soil to a depth of 0.25 m. In the remaining part of this paper all EC_a measurement values refer to the EC_a at 25 °C.

Modeling the compacted layer

The cumulative response of the EM38-MK2 (expressed in % of the measured signal) from a layered soil volume below a depth z (in m) beneath the sensor is given by (McNeill, 1980), both for the vertical $[R_v(z)]$ and the horizontal orientations $[R_h(z)]$:

$$R_v(z) = \left[4.(z/s)^2 + 1\right]^{-0.5} \quad (2)$$

$$R_h(z) = \left[4.(z/s)^2 + 1\right]^{0.5} - 2.z/s \quad (3)$$

where s is the inter-coil (transmitter-receiver) spacing. These response functions allow modeling the relationship between the conductivity of a soil layer and EC_a. For a paddy field,

Figure 1 (a) Mobile soil sensing system with: (i) laptop (protected by a plastic sheet), (ii) GPS antenna, (iii) waterproof sensor housing with an EM38-MK2 inside, (iv) floating platform and (v) tractor; (b) EM38-MK2.

we can define the depth to the interface between the puddled layer and the compacted layer as z_{pp}, and the depth to the interface between the compacted layer and the soil material below it as z_{ppb}. Then the thickness of the compacted layer can be calculated as $z_{ppb}-z_{pp}$. The cumulative response from the puddled layer, compacted layer and the uncompacted soil material beneath can be calculated as $1-R(z_{pp})$, $R(z_{pp})-R(z_{ppb})$ and $R(z_{ppb})$, respectively. For the 10 locations on transect AB, the z_{ppb} observations can be coupled with their nearest EC_a measurements. Then the predicted z^*_{ppb} can be modeled by solving a system of non-linear equations, given the apparent conductivity values of the puddled layer ($EC_{a,p}$), of the compacted layer ($EC_{a,pp}$) and of the uncompacted soil beneath ($EC_{a,ppb}$):

$$EC_a = [1 - R(z_{pp})].\ EC_{a,p} + [R(z_{pp}) - R(z^*_{ppb})].\ EC_{a,pp} + R(z^*_{ppb}).\ EC_{a,ppb} \quad (4)$$

The automated FSOLVE function based on the Levenberg–Marquardt algorithm (Marquardt, 1963) in the Matlab computing environment (MathWorks, Natick, MA, USA) was used. The sum of the squared differences between z_{ppb} and z^*_{ppb} was minimized in order to fit the theoretical relationship to the z_{ppb} and EC_a data using:

$$\sum_{i=1}^{n} [z_{ppb} - z^*_{ppb}(i)]^2 = \min \quad (5)$$

with n being the number of observations. The modeling parameters $EC_{a,pp}$ and $EC_{a,ppb}$ were iteratively adjusted to obtain the smallest sum of the squared differences between z_{ppb} and z^*_{ppb}. Detailed description of the methodology can be found in Saey *et al*. (2008, 2009b).

An independent validation can be performed to evaluate the predictive quality of the model. The Pearson correlation coefficient (r), mean estimation error (MEE) and root mean square estimation error (RMSEE) were used as the validation indices. When r is close to 1, the z_{ppb} and z^*_{ppb} have a strong positive association. The bias of the model becomes low and the accuracy of the model becomes high when MEE and RMSEE, respectively approach 'zero'. The MEE and RMSEE were obtained as:

$$MEE = \frac{1}{n}\sum_{i=1}^{n} [z^*_{ppb}(i) - z_{ppb}(i)] \quad (6)$$

$$RMSEE = \sqrt{\frac{1}{n}\sum_{i=1}^{n} [z^*_{ppb}(i) - z_{ppb}(i)]^2} \quad (7)$$

with i being the number of validation observations. At each location, depth of the compacted layer was observed by PR measurements and the observed depths were compared with the model predictions.

Water percolation measurements

A transect CD was laid out covering the length of the field in N-S orientation and 18 locations were selected (Figure 3c). At each location, the steady state infiltration was measured three times within 1 m^2 with a double ring infiltrometer (0.30 m inner ring diameter and 0.45 m outer ring) by measuring the decrease in water level in the inner ring as a function of time. The insertion depth of the rings was about 0.16 m and the water level outside and inside the rings was similar. In flooded field condition, the final infiltration rate would actually refer to the flux percolation rate, which indeed equals the hydraulic conductivity. Measurements continued for 2 days to check the hydraulic gradient which became unity. Under water saturated paddy field conditions, these measurements indicate the permeability of the least conductive layer i.e. the compacted layer.

Results and discussion

Bulk density measurements

Table 1 gives the descriptive statistics together with a statistical comparison of the mean values of the soil bulk density for the three depth intervals: 0–0.15, 0.15–0.30 and 0.30–0.45 m. The smallest mean bulk density values (1.33 Mg/m^3) were found within 0–0.15 m and the largest (1.63 Mg/m^3) within 0.15–0.30 m; the value (1.46 Mg/m^3) was intermediary for the 0.30–0.45 m. The differences of the mean bulk density values were significant at $\alpha = 0.05$ for the three depth intervals. This indicated the clear difference among the three soil layers where the 0.15–0.30 m layer corresponded to the compacted layer. However, the large variation within this layer (between 1.42 and 1.79 Mg/m^3) indicated that soil bulk density also varied the most within this layer. These values are similar to those found by Islam *et al*. (2011).

Table 1 Descriptive statistics and mean comparison of soil bulk densinty (in Mg/m^3) values observed at 10 points on a calibration transect AB

Soil depth (m)	Mean* (Mg/m^3)	Minimum (Mg/m^3)	Maximum (Mg/m^3)	CV (%)
0–0.15	1.33	1.19	1.41	5.9
0.15–0.30	1.63	1.42	1.79	7.3
0.30–0.45	1.46	1.41	1.63	2.9

PR, penetration resistance; CV, coefficient of variation. *Means are significantly different ($P = 0.05$) according to Fisher's least significant difference test.

EC_a survey measurements

Table 2 contains the descriptive statistics of the EC_a survey measurements across the whole field. The mean EC_a values were the largest for the intermediate DOIs: 51 and 54 mS/m for H1 and V.5, respectively. However, the means were lower for both the shallowest and the deepest DOIs: 44 mS/m for H.5 and 39 mS/m for V1. These EC_a measurements indicate that the shallow and deep soil material is less conductive than the soil material at intermediary depth. The relative response curves are given by McNeill (1980, 2008) and shown in Figure 2. From Figure 2 it is clear that H.5 and H1 respond mostly to the puddled layer i.e. soil close to the surface. On the other hand, V.5 reflects the intermediary depth referring to the compacted layer and V1 is mainly influenced by the soil below the compacted layer.

The small variances of EC_a for the H.5 and V1 coil orientations (Table 2) indicate that both the puddled layer and the soil below the compacted layer had limited variability. On the contrary, the largest variance of EC_a for the V.5 coil orientation indicates that the compacted soil layer accounted for the largest EC_a variation.

All the EC_a data sets were interpolated with ordinary kriging (Goovaerts, 1997) to create four EC_a maps with a resolution of 0.5 m by 0.5 m. All four variograms were best modelled by an omnidirectional spherical model and the kriged maps are given in Figure 3.

The four EC_a maps in Figure 3 show similar patterns of fluctuating values across the field without a systematic trend. However, the shallow EC_a measurements (Figure 3a,b,c) indicate a larger variability than the deep measurement (Figure 3d). Moreover, the relative response functions in Figure 2 showed that measurements obtained with the shallow measuring coil configuration in V.5 are insensitive to the soil close to the surface but receives a dominant influence from the soil depth, which is typically compacted in paddy fields. Hence, it can allow detection of conductivity variations in the compacted layer of paddy fields. For a given volume, soil compaction results in a larger amount of small soil pores because of closer packing of soil particles. The finer the soil pores are the larger the concentrations of the pore solution becomes, resulting in larger electrical conductivity values.

Table 2 Descriptive statistics of EC_a variables

EC_a variable	DOI (m)	*n*	Mean (mS/m)	Minimum (mS/m)	Maximum (mS/m)	CV $(mS/m)^2$
H.5	0.38	35 673	44	28	60	30.3
H1	0.75	35 673	51	29	75	62.7
V.5	0.75	35 370	54	32	77	62.6
V1	1.5	35 370	39	20	59	46.8

n, number of observations; CV, coefficient of variation.

Relationship between EC_a, bulk density and PR

Table 3 gives the correlation coefficients, *r* between co-located EC_a, bulk density and PR for the three soil depth intervals. PR data were stratified for the three soil depth intervals of 0–0.15, 0.15–0.30 and 0.30–0.45 m. The average was calculated for each depth interval and used for correlation. For all depth intervals, the correlation between EC_a in the V.5 coil configuration and bulk density were stronger than the relationship between EC_a in other coil configurations and bulk density values. However, the very strong relationship between V.5 and PR, both measured under paddy growing conditions, is clear. This points out that the V.5 measurements are appropriate for detecting differences in soil compaction depth. Therefore, among the four EC_a data sets, the EC_a in the V.5 coil configuration was selected, and in the following parts of this paper all EC_a values refer to the EC_a obtained with the V.5 configuration.

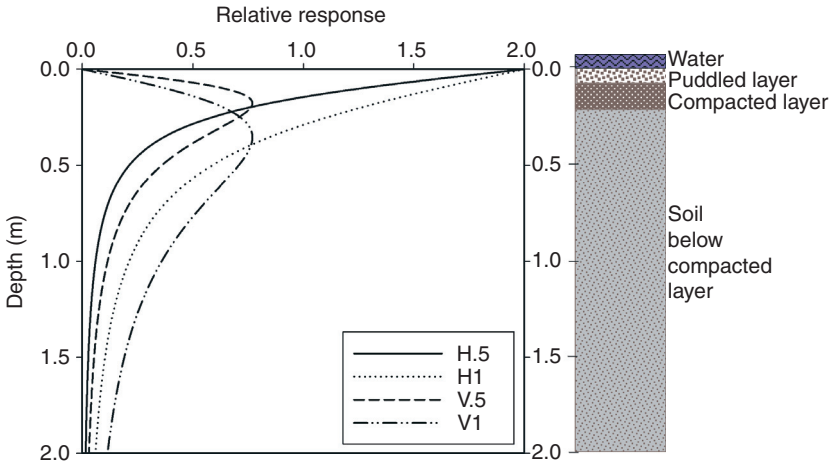

Figure 2 Relative response of the four coil configuration as a function of depth (m) for the EM38-MK2 in horizontal (.5H and 1H) and vertical (.5V and 1V) configurations with 0.5 and 1 m transmitter-receiver coil separation (left figure) and a typical layered paddy field model showing the different soil layers with indication of approximate layer depths beneath a standing water layer of few centimetres (right figure).

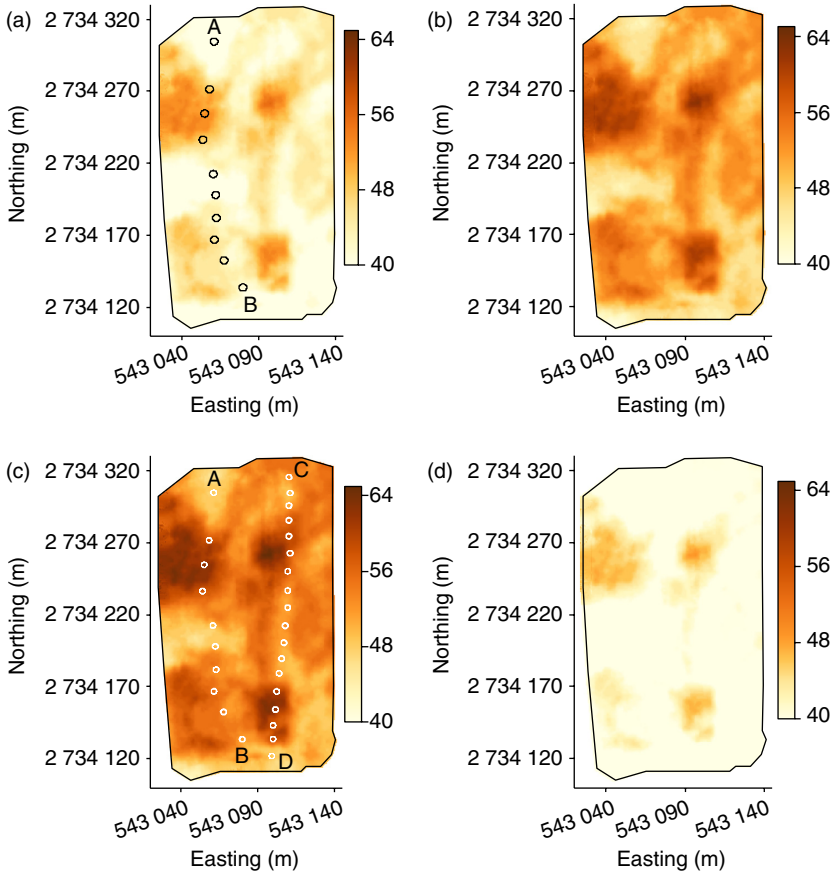

Figure 3 Interpolated apparent electrical conductivity (EC_a) in mS/m using 0.5 and 1.0 m intercoil distances of the EM38-MK2 in both horizontal and vertical orientations: (a) EC_a with H.5, (b) EC_a with H1, (c) EC_a with V.5 and (d) EC_a with V1 coil configuration. AB (n = 10) and CD (n = 18) are two transects for calibration and validation respectively, showing measurement locations as circles.

Table 3 Pearson correlation coefficient (r) between EC_a, soil bulk density and penetration resistance

	Bd_15	Bd_30	Bd_45	PR_15	PR_30	PR_45
H0.5	0.24	0.64	0.61	0.19	0.72	0.75
H1	0.23	0.64	0.61	0.16	0.81	0.76
V.5	0.013	0.71	0.63	0.13	0.89	0.83
V1	0.002	0.66	0.56	0.19	0.73	0.75

Bd, bulk density for a depth interval; PR, average penetration resistance for a depth interval; _15, _30 and _45, measurements obtained from soil depth intervals of 0–0.15, 0.15–0.30 and 0.30–0.45 m, respectively (n = 10).

Penetration resistance measurements of saturated paddy soils are useful as an indicator of soil compaction. The penetrometer could measure the relative soil compaction at much smaller depth intervals under paddy growing conditions than typical soil bulk density samples could be obtained under dry field conditions. Therefore, the PR measurements at the 10 locations along transect AB were used to observe the depth of the compacted layer. Figure 3a shows that these locations covered a wide range of EC_a including both large and small EC_a values. For the same locations, Figure 4 shows the PR measurements with respect to soil depth. The pattern is clearly visible: soil compaction gradually increased and reached a maximum PR with depth (z_{pp}), thereafter, the values remained relatively unchanged (i.e. stable PR values) over a depth range of few to tens of centimeters. This stability indicated that the degree of compaction was similar everywhere within the compacted soil layer. With further increase in depth the PR values decreased. Therefore, the distinction between the uncompacted soil layers and depth of the compacted layer z_{ppb} is clearly observable. The first and second derivatives of PR with respect to depth were determined (Isaac *et al.*, 2002) to numerically identify the sharp changes and peaks in the PR data, which are indicative of the soil layers having distinct compaction differences. z_{ppb} revealed to be highly variable along transect AB.

The compacted layer

Using the direct soil EC meter and PR measurements, 10 coupled conductivity and depth measurements along transect AB were obtained from the puddled upper soil layer. The instrument measures the total (bulk) soil conductivity but in contrast to the EM38-MK2, the individual measurements

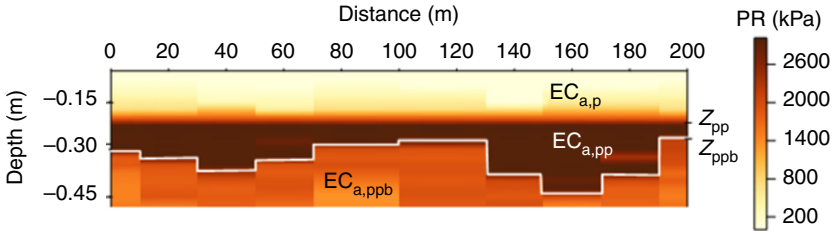

Figure 4 The penetration resistance (PR) measurements along transect AB (n = 10); the modeling parameters $EC_{a,p}$ and z_{pp} are constants, where $EC_{a,p}$ is the conductivity of the puddled upper layer, and z_{pp} is the depth to the interface between the puddled layer and the compacted layer; $EC_{a,pp}$ and $EC_{a,ppb}$ are conductivities of the compacted and the uncompacted layer beneath; z_{ppb} presented as solid line is the depth to the interface between the compacted and the uncompacted layer.

cover a limited elliptical soil volume around the probe. The mean conductivity was 21.3 mS/m ($EC_{a,p}$) with a standard deviation (SD) of 0.8 mS/m and the mean z_{pp} was 0.16 m with a SD of 0.01 m. These low values of SD indicated a limited variability and therefore, allowed us to take the $EC_{a,p}$ and z_{pp} parameters being constant along the study site. Next, the 10 z_{ppb} observations of transect AB were compared with their nearest EC_a measurements recorded with the EM38-MK2 (Figure 5). Figure 6 shows the theoretical EC_a – depth relationship fitted to the z_{ppb} and EC_a data points by minimizing the sum of the squared differences between z_{ppb} and z^*_{ppb} deduced from equation (4). At each measurement point, iterative adjustment resulted in optimal $EC_{a,pp}$ and $EC_{a,ppb}$ values of 90.6 and 35.6 mS/m with a R^2 value of 0.89. Then z^*_{ppb} was modeled by using equations (2) and (4) given the measured EC_a (from EM38-MK2), the constant $EC_{a,p}$ and z_{pp}; and fitted $EC_{a,pp}$ and $EC_{a,ppb}$.

Figure 7 shows the interpolated map of the modeled z^*_{ppb} values of the field. It is clear from Figure 7 that there are several locations with small z^*_{ppb} values that would require due attention during land preparation in terms of soil water management. Due to a lack of EC_a values < 43 mS/m (Figure 6) the accuracy of the model cannot be determined below this value and hence z^*_{ppb} are very uncertain. However, the accuracy of the model to predict compaction depth was evaluated. Therefore, a validation transect (CD) was laid out (Figure 3c) along which 18 observation locations separated by approximately 10 m were selected. A strong correlation (r = 0.87) between predicted (z^*_{ppb}) and measured depth (z_{ppb}) with low RMSEE and MEE values of 0.03 and 0.04 m, respectively indicated that the methodology used was highly accurate with a low bias in predicting z^*_{ppb} (Figure 8).

The modeling methodology described in this study justifies the ability of the soil sensing system to predict the interface between contrasting soil layers continuously across a field using a multi-receiver EMI instrument. Because two different interfaces in a paddy field imply a three-layered soil model, this model requires simplification. Therefore, the conductivity of one soil layer is fixed across the study site.

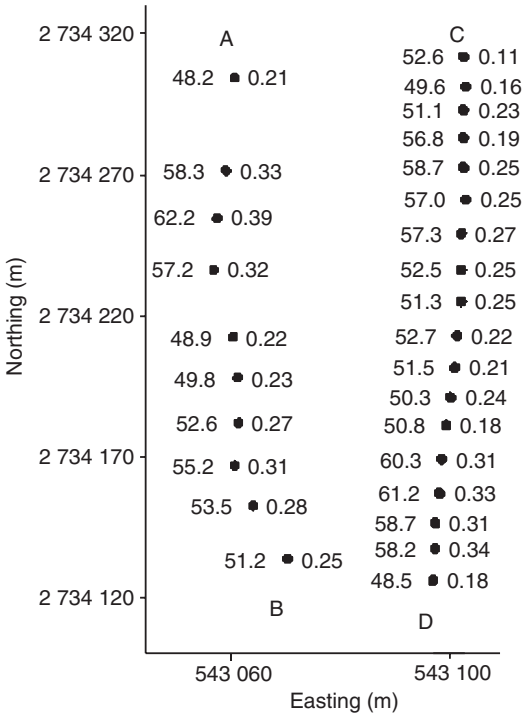

Figure 5 The co-located EC_a and z_{ppb} (the depth to the interface between the compacted and the uncompacted layer) measurements along transect AB (n = 10) and CD (n = 18), showing measurement locations as circles; numeric values to the left of a circle is the EC_a and to the right of a circle is the z_{ppb} at that location.

By taking a limited number of calibration observations, the EC_a of the puddle layer can be estimated by the average value of that layer.

Compacted layer thickness and water percolation

A compacted soil layer should be able to maintain a wet condition in the paddy field by decreasing water losses beyond the rooting zone. Therefore, the percolation measurements taken at 18 locations along the validation transect CD were used to interpret the thickness differences

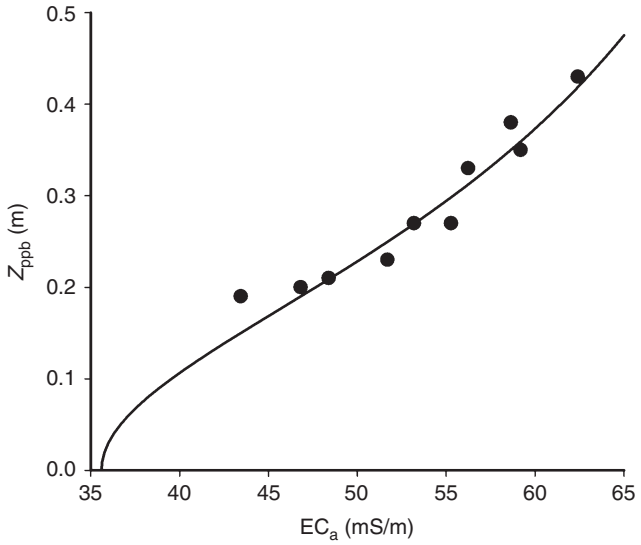

Figure 6 z_{ppb} as a function of EC_a along the transect AB with fitted cumulative depth response curve for the EM38-MK2 in 0.5 m intercoil distance in vertical orientation (n = 10).

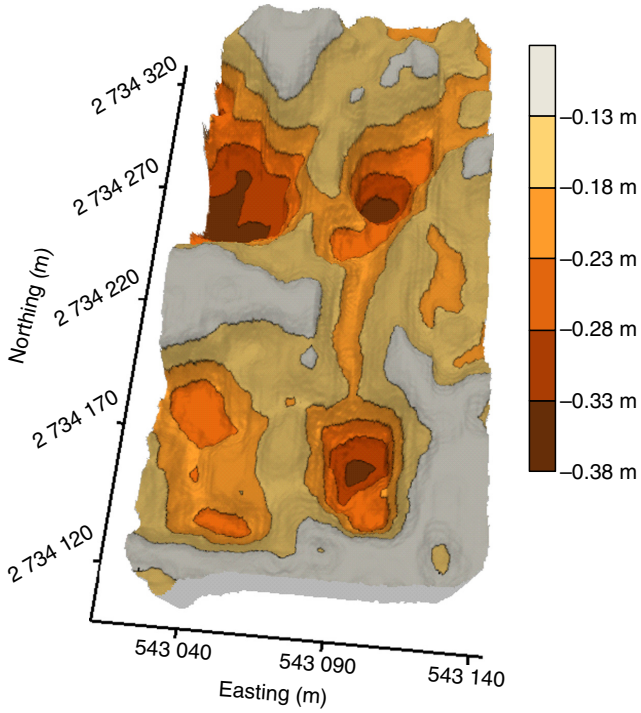

Figure 7 Interpolated z^*_{ppb} (predicted depth to the interface between the compacted soil layer and the soil beneath the compacted layer) map of the field.

of the compacted layer. Percolation rates ranged from 8 to 32 mm/day with a mean of 18.3 mm/day. Figure 9 shows the scatter plot of the percolation measurements and the modeled thickness of the compacted layer calculated as

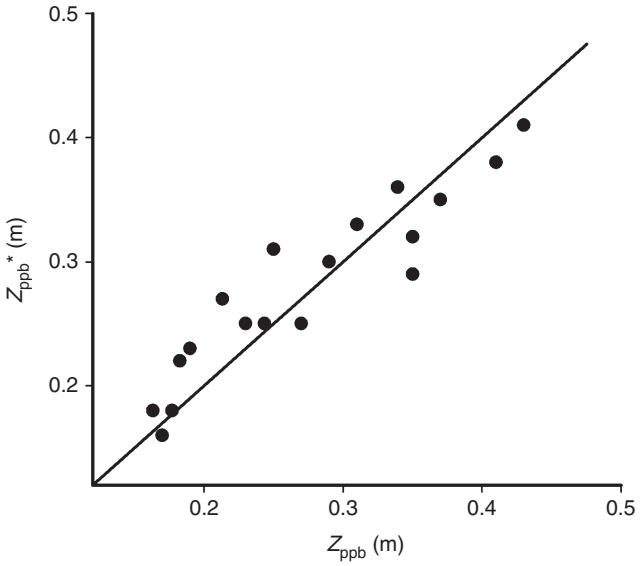

Figure 8 Predicted (z^*_{ppb}) and observed (z_{ppb}) depth to the interface between the compacted soil layer and the soil beneath the compacted layer along transect CD using 18 observations, with the diagonal solid line representing agreement between prediction and observation.

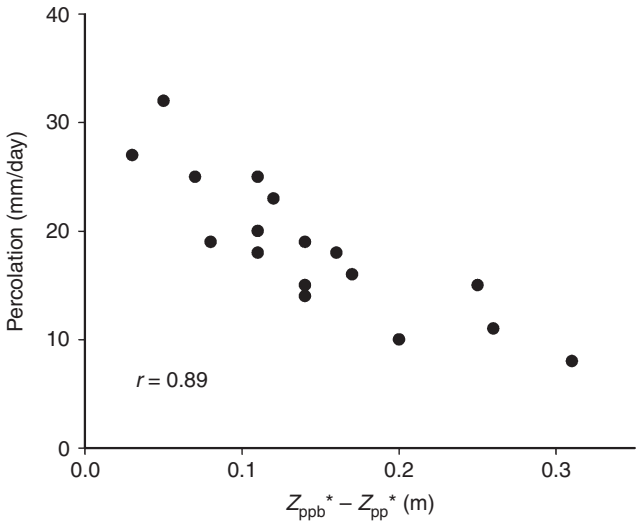

Figure 9 Predicted compacted layer thickness ($z^*_{ppb} - z^*_{pp}$) and water percolation measurements observed on 18 locations along the validation transect (CD).

$z^*_{ppb} - z^*_{pp}$ along transect CD. The Pearson correlation coefficient, r between these two was 0.89 and the relationship was inverse (Figure 9). At locations where $z^*_{ppb} - z^*_{pp}$ is small, there is a higher risk of percolation losses, which are usually accompanied by losses of nutrients. Large values of $z^*_{ppb} - z^*_{pp}$ can decrease this risk. Therefore, it is clear that the thickness of the compacted layer as predicted by the model also had a strong link to percolation losses.

A multi-receiver EMI instrument with at least four coil configurations expands the possibilities to perform depth sounding with a limited amount of calibration observations. The approach of predicting the compacted layer thickness is generally applicable for a three-layered soil, which is common for paddy fields assuming constant conductivity values for the layers. Therefore, this methodology seems to be appropriate for smaller paddy fields, as is common in Asian farming systems but it might require further investigation before making recommendations for larger fields.

Conclusions

The thickness of the compacted soil layer was not uniform within the paddy field. The EMI based sensing system proved to be successful in detailed measuring of the soil layers within a paddy field under growing conditions. Measurements with the EM38-MK2 in the vertical orientation with 0.5 m transmitter-receiver coil spacing are appropriate for investigating the compacted layer in paddy fields. Hence, the thickness differences of this soil layer could be modeled accurately. Although, this compacted layer is the least permeable layer, the layer thickness was inversely related to water percolation losses.

In the conditions for crop production, losses of nutrients such as nitrogen and phosphorus, together with the percolated water can have environmental consequences by polluting the ground water. To tackle this, delineation of compaction zones based on detailed EMI measurements and compacted layer modeling could be helpful. The delineated zones could be considered as separate units for soil water management. Two approaches can be suggested: adjustment of puddling during land preparation and bunding of the zones along the boundaries before water application.

To conclude, the combination of high-density sensor measurements coupled with limited direct observations is able to measure the variability of the compacted layer of a paddy field. This offers new opportunities for precise soil management in paddy rice cultivation system.

References

ASABE standards 2011. *S313.3. Soil cone penetrometer*. ASABE, St. Joseph, MI.

Brammer, H. 1981. *Reconnaissance soil survey of Dhaka district*, Revised edn, pp. 6–19. Soil Resources Development Institute, Dhaka, Bangladesh.

Brammer, H. 1996. *The geography of the soils of Bangladesh*, pp. 25. The University Press Limited, Dhaka, Bangladesh.

Brevik, E.C. & Fenton, T.E. 2004. The effect of changes in bulk density on soil electrical conductivity as measured with the Geonics EM-38. *Soil Survey Horizons*, **45**, 96–102.

De Datta, S.K. 1981. *Principles and practices of rice production*, pp. 618. Wiley-Interscience, New York.

Goovaerts, P. 1997. *Geostatistics for natural resources evaluation*. Oxford University Press, New York.

Hoefer, G., Bachmann, J. & Hartge, K.H. 2010. Can the EM38 probe detect spatial patterns of subsoil compaction? In: *Proximal soil sensing, progress in soil science 1* (eds R.A. Viscarra Rossel, A.B. McBratney & B. Minasny), pp. 265–273. Springer, Netherlands.

Isaac, N.E., Taylor, R.K., Staggenborg, S.A., Schrock, M.D. & Leikam, D.F. 2002. Using cone index data to explain yield variation within a field. *Agricultural Engineering International: The CIGR Journal of Scientific Research and Development*, **4**, 19–33.

Islam, M.M. & Van Meirvenne, M. 2011. FloSSy: a floating sensing system to evaluate soil variability of flooded paddy fields. In: *Proceedings of the 8th European Conference on Precision Agriculture* (ed. J.V. Stafford), pp. 60–66. University of Life Sciences, Prague, Czech Republic.

Islam, M.M., Cockx, L., Meerschman, E., De Smedt, P., Meeuws, F. & Van Meirvenne, M. 2011. A floating sensing system to evaluate soil and crop variability within flooded paddy rice fields. *Precision Agriculture*, **12**, 850–859.

Islam, M.M., Meerschman, E., Saey, T., De Smedt, P., Van De Vijver, E. & Van Meirvenne, M. 2012. Comparing apparent electrical conductivity measurements on a paddy field under flooded and drained conditions. *Precision Agriculture*, **13**, 384–392.

Kukal, S.S. & Sidhu, A.S. 2004. Percolation losses of water in relation to pre-puddling tillage and puddling intensity in a puddled sandy loam rice (*Oryza sativa*) field. *Soil and Tillage Research*, **78**, 1–8.

Marquardt, D. 1963. An algorithm for least-squares estimation of nonlinear parameters. *SIAM Journal on Applied Mathematics*, **11**, 431–441.

Martinez, G., Vanderlinden, K., Ordonez, R. & Muriel, J.L. 2009. Can apparent electrical conductivity improve the spatial characterization of soil organic carbon? *Vadose Zone Journal*, **8**, 586–593.

McDonald, A.J., Riha, S.J., Duxbury, J.M., Steenhuis, T.S. & Lauren, J.G. 2006. Soil physical responses to novel rice cultural practices in the rice-wheat system: comparative evidence from a swelling soil in Nepal. *Soil and Tillage Research*, **86**, 163–175.

McNeill, J.D. 1980. *Electromagnetic terrain conductivity measurement at low induction numbers*. Technical Note TN-6. Geonics Limited, Missisauga, Ontario, Canada.

McNeill, J.D. 2008. *EM38-MK2 ground conductivity meter operating manual*. Geonics Limited, Missisauga, Ontario, Canada.

Motavalli, P.P., Andersob, S.H., Pengthamkeerati, P. & Gantzer, C.J. 2003. Use of cone penetrometer to detect the effects of compaction and organic amendments in claypan soils. *Soil and Tillage Research*, **74**, 103–114.

Perumpral, J.V. 1987. Cone penetrometer applications: a review. *Transactions of the American Society of Agricultural Engineers*, **30**, 939–944.

Reintam, E., Trükmann, K., Kuht, J., Nugis, E., Edesi, L., Astover, A., Noormets, M., Kauer, K., Krebstein, K. & Rannik, K. 2009. Soil compaction effects on soil bulk density and penetration resistance and growth of spring barley (*Hordeum vulgare* L.). *Acta Agriculture Scandinavica B*, **59**, 265–272.

Rhoades, J.D., Manteghi, N.A., Shouse, P.J. & Alves, W.J. 1989. Soil electrical conductivity and soil salinity: new formulations and calibrations. *Soil Science Society of America Journal*, **53**, 433–439.

Rhoades, J.D., Chanduvi, F. & Lesch, S.M. 1999. *Soil salinity assessment: methods and interpretation of electrical conductivity measurements*. FAO Rep. 57. FAO, Rome, Italy.

Saey, T., Simpson, D., Vitharana, U., Vermeersch, H., Vermang, J. & Van Meirvenne, M. 2008. Reconstructing the paleotopography beneath the loess cover with the aid of an electromagnetic induction sensor. *Catena*, **74**, 58–64.

Saey, T., Van Meirvenne, M., Vermeersch, H., Ameloot, N. & Cockx, L. 2009a. A pedotransfer function to evaluate the soil profile textural heterogeneity using proximally sensed apparent electrical conductivity. *Geoderma*, **150**, 389–395.

Saey, T., Simpson, D., Vermeersch, H., Cockx, L. & Van Meirvenne, M. 2009b. Comparing the EM38DD and DUALEM-21S sensors for depth-to-clay mapping. *Soil Science Society of America Journal*, **73**, 7–12.

Saey, T., Islam, M.M., De Smedt, P., Meerschman, E., Van De Vijver, E., Lehouck, A. & Van Meirvenne, M. 2012. Using a multi-receiver survey of apparent electrical conductivity to reconstruct a Holocene tidal channel in a polder area. *Catena*, **95**, 104–111.

Sheets, K.R. & Hendrickx, J.M.H. 1995. Non-invasive soil water content measurement using electromagnetic induction. *Water Resources Research*, **31**, 2401–2409.

Simbahan, G.C., Dobermann, A., Goovaerts, P., Ping, J. & Haddix, M.L. 2006. Fine resolution mapping of soil organic carbon based on multivariate secondary data. *Geoderma*, **132**, 471–489.

Sudduth, K.A., Hummel, J.W. & Birrell, S.J. 1997. Sensors for site-specific management. In: *The state of site-specific management for agriculture* (eds F.J. Pierce & E.J. Sadler), pp. 183–210. ASA-CSSA-SSSA, Madison, WI.

Sudduth, K.A., Kitchen, N.R., Wiebold, W.J., Batchelor, W.D., Boller, G.A., Bullock, D.G., Clay, D.E., Palm, H.L., Pierce, F.J., Schuler, R.T. & Thelen, K.D. 2005. Relating apparent electrical conductivity to soil properties across the north-central USA. *Computers and Electronics in Agriculture*, **46**, 263–283.

Triantafilis, J., Laslett, G.M. & McBratney, A.B. 2000. Calibrating an electromagnetic induction instrument to measure salinity in soil under irrigated cotton. *Soil Science Society of America Journal*, **64**, 1009–1017.

Van Meirvenne, M., Islam, M.M., De Smedt, P., Meerschman, E., Van De Vijver, E. & Saey, T. 2013. Key variables for the identification of soil management classes in the Aeolian landscapes of north–west Europe. *Geoderma*, **199**, 99–105.